

## Removal of Uranium from aqueous solution using potato peels as bio-sorbent

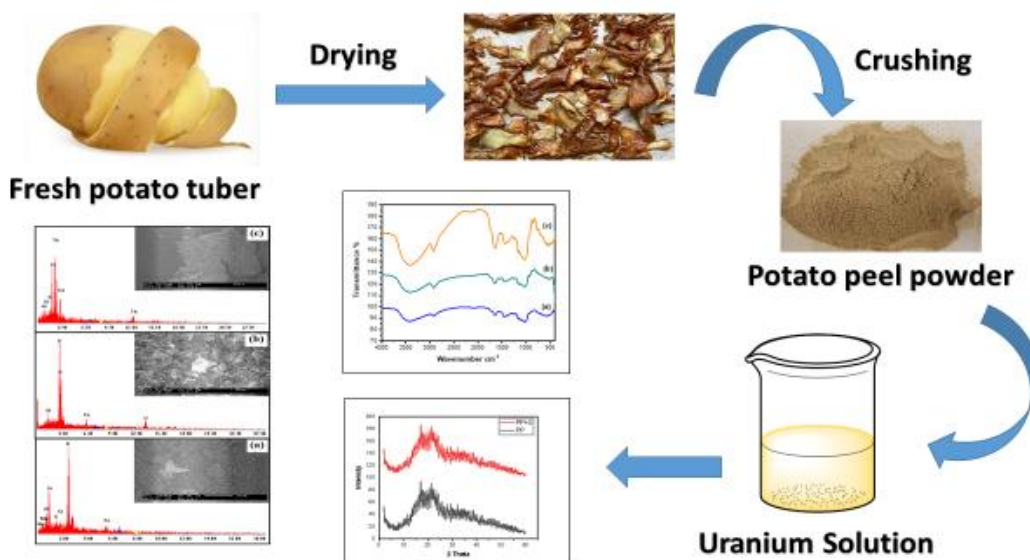
Aesha A. Mohamed, Rania A. Roshdi, Hend M. Salem and  
Aziza I.L. Abd El Fatah

Nuclear Materials Authority, P. O. Box 530 Maadi, Cairo, Egypt  
Corresponding Author: Hend M. Salem

### ABSTRACT

Potato peel (PP) as bio-residue from the food processing industry used as novel uranium adsorbents, applied for studying the adsorption of uranium from aqueous solution. In batch studies, the adsorption of uranium (U, VI) from aqueous solutions onto PP was examined. From FTIR, PP represented function group (carboxyl, amino, and hydroxyl) on its surface lead to improve its adsorption. Moreover, Chloride media's showed the best adsorption efficiency for U (VI) reached up to 95.75 by PP. Also, the adsorption was studied at various temperatures, uranium concentrations, times, and pH values and the results showed that pH 4 was the best for uranium adsorption onto PP. The adsorption of uranium increased and reached to equilibrium times at 60 minutes with adsorption capacity of 19.25 mg/g. Furthermore, the bio-sorption process fit the Langmuir isotherm model well, and the kinetics were described by a pseudo-second-order rate equation, specifically. FTIR, ESEM-EDX, XRD, particle size, and zeta potential techniques were used to confirm the uptake of uranium by PP. Ultimately, the results of this study showed that PP may be a practical, quick, affordable, and effective way to extract uranium from an acidic monazite mineral aqueous solution.

### GRAPHICAL ABSTRACT



**Keywords:** kinetics' Thermodynamics' Potato peels (PP)' Sorption isotherms' Adsorption' Characterization and Uranyl ion U(VI).

Received 15 June., 2025; Revised 28 June., 2025; Accepted 30 June., 2025 © The author(s) 2025.  
Published with open access at [www.questjournals.org](http://www.questjournals.org)

## I. INTRODUCTION

The Earth's crust contains uranium, it can be discovered in nature in complicated ores including uranophane, pitch-blende, autunite, carnotite, and torbernite. The concentration of uranium in the Earth's crust is around 2.8 mg/kg. However, uranium released into the environment is a result of a number of human actions, including the testing of nuclear weapons, mineral mining, and the usage of phosphate fertilizers. Uranium removal from contaminated regions is therefore essential for following regulatory requirements and maintaining environmental safety, Alqadami et al. [1].

Adsorption Abdi S, et al. [2], membrane filtration Ding S et al. [3], ion exchange Chen QY, et al. [4], and electro-dialysis have all been used to eliminate uranium from groundwater Onorato C et al. [5]. Among these approaches adsorption is widely used due to its low cost, high efficiency, easy-to-operate and maintenance Shasha Yang et al. [6].

The increasing amount of food waste throughout the world is becoming a major problem for waste management plants. The food waste produced amounts to 1.3 million tons a year. This is a resource that could be used for production of new products. Bio-economy is a method that can help achieve production of value-added products that use local resources and waste to manufacture products efficiently. This by-product causes environmental pollution due to decomposition, Ecaterina Matei et al. [7].

These days, the steadily rising amounts of trash have a significant impact on the ecosystem's health and the quality of life. The agro-food business produces valuable materials with well-known potential on a global scale in the form of agri-food wastes. These have naturally occurring bioactive chemicals that are used in the food, medicine, and cosmetics industries as well as in the production of bioethanol, energy, and compost Ecaterina Matei et al [7]. But given the volume of agri-food wastes associated with financial strain on resource sustainability, greater consideration needs to be given to the use and recycling strategies for agro-industrial waste, Yusuf et al [8]. Thus, potato waste represents promising cheap resources and its recovery and recycling within the food chain could be a sustainable strategy to address the present challenges of the industrialized world.

Noting that potato peels are the second-most-wasted food ingredient, according to Jagtap et al [9]. Its powder is utilized in the food processing industry to increase sustainability. Potato peels are a zero-value by-product that are produced in large quantities during processing. Because potato peels contain a high level of dietary fiber, the industry finds it vital to use them throughout the processing of potatoes Selvendran et al. [10]. Furthermore, food byproducts like potato peel have essential organic matter. It has high levels of polyphenols, minerals, vitamins, amino acids, dietary fiber, and carbohydrates. It is the primary byproduct of the potato processing industry and has the potential to be valued as a source of bioactive and functional chemicals, with phenolic acids receiving special attention. Potato wastes have been the subject of significant research. After a preliminary treatment and showed good removal efficiency for the heavy metals. Kyzas et al. [11-15]. Yet, acclimation of these peels would represent an environmental burden. Recycling of these wastes into a low-cost, versatile adsorbent for the removal of Uranium to get rid of these wastes and simultaneously clean wastewater. In the present study, we used PP by product contain high level of organic compound without any modification as adsorption system to study its effect on the adsorption for removal uranium from aqueous solutions using batch technique. Also, predict the optimizing conditions at different of pH, time, uranium concentration and temperature.

## II. EXPERIMENTAL

### Preparation of adsorbent

The uncooked potato peels came from a nearby restaurant's garbage. After giving the materials a thorough wash to get rid of any soil left on the peel's surface, they were given another washing with distilled water. By keeping the peels in a lab oven at 50°C, the water content in the peels was totally removed. The dried material was then mashed using a commercial mill. Figure 1 illustrates the material's average particle size, which ranged from -0.125 to 1.00 mm. The bio-removal of uranium from aqueous solutions under several conditions, including pH, temperature, and contacting time, was investigated for all peel types.

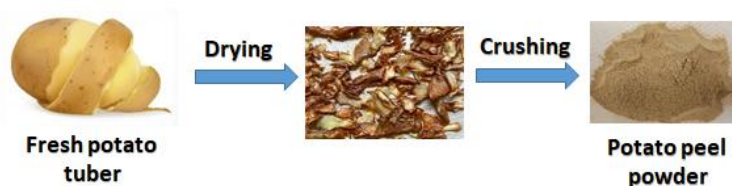


Figure 1: Preparation of potato peel powder (PPP)

The antioxidant properties of potato peels are attributed to their diverse polyphenols and phenolic acids, while lipids and fatty acids demonstrated antibacterial properties. On a dry basis, it also comprises 25% starch, 30% non-starch polysaccharide, 18% protein, 20% acid-soluble and acid-insoluble lignin, 1% fat, and 6% ash. Triglycerides, alcohols, sterol esters, and long-chain fatty acids are all found in the lipid fraction. Furthermore, potato cell walls have been shown to contain lignin units. Potato peels have a high starch content (52% dry weight), but only a little amount (0.6% dry weight) of fermentable reducing sugar. Since it is not physically feasible to ferment potato peels for this purpose, the concentration of fermentable reducing sugar must first be increased by the breakdown of carbohydrates, either enzymatically or acidically. Potato peel elements include C ( $43.78 \pm 0.15$ ), H ( $5.96 \pm 0.12$ ), N ( $4.06 \pm 0.01$ ), and O ( $46.21 \pm 0.28$ ) (in percentage dry basis). Potato peels are 6.5 in pH and have a C/N ratio of 10.7. Potato peels have a calorific value of  $17.37 \pm 0.38$  (MJ/kg). The potato peel extract contains a variety of phenolic acids, including p-hydroxybenzoic acid (82.0–87.0 mg/100 g), p-coumaric acid (41.8–45.6 mg/100 g), vanillic acid (43.0–48.0 mg/100 g), caffeic acid (278.0–296.0 mg/100 g), gallic acid (58.6–63.0 mg/100 g), and protocatechuic acid (216.0–256.0 mg/100 g) Ahsan et al. [16].

### **Instruments**

In situ studies are carried out in batches using a stock solution of uranyl nitrate hexahydrate ( $\text{UO}_2(\text{NO}_3)_2 \cdot 6\text{H}_2\text{O}$ ) diluted to a concentration of 1000 ppm. Using Arsenazo I as an indicator. The functional group's study was completed using the a Nexeus-Nicolite model 640-MSA spectrometer from Bruker Optik GmbH in Ettlingen, Germany, which uses attenuated total reflectance Fourier transform infrared (ATR-FTIR) technology with a resolution of  $0.5 \text{ cm}^{-1}$  across a range of  $4000 - 400 \text{ cm}^{-1}$  produced in KBr discs. The morphology of the samples surface was examined utilizing SEM of a JEOL-JSM-5600LV SEM, UK, after coated with gold for 3 min. Samples were examined with X-ray type PW 3710 = 31 from Philips, Bruker, Germany. All the diffraction patterns were investigated at room temperature and diffractometer using monochromatic Ni-filtered Cu K alpha radiation at 40 kV and 30 mA. Scan range ( $2\theta$ ), 4 - 908. UV-vis spectrophotometer (UV-1 601 model Shimadzu) was used to measure uranium at 596 nm. An isothermal circulator, (Lindberg Blue, USA) was used for batch studies, and it ran at 300 rpm. The digital pH meter of the Ino LabWTW type was used to measure the pH. NICOMP 380 ZLS, Dynamic light scattering (DLS) instrument (PSS, Santa Barbara, CA, USA), using the 632 nm line of a HeNe laser as the incident light with angle  $90^\circ$  and Zeta potential with external angle  $18.9^\circ$ . Nanomaterial Investigation Lab., Central Laboratory Network (CLN), National Research Centre (NRC).

### **Adsorption studies**

Adsorption capacity experiments were carried out in a 100 ml Erlenmeyer flask containing 10 ml of uranium solution (25-400  $\text{mgL}^{-1}$ ). Adsorbent (0.01-1.15g) was used, and mixing periods (5-90 min) were chosen within a pH range of 1-5. The following headings provide more information about the specifics of the supplies, tools, processes, and methods used in the current investigation: The percent removal of uranium from solution was calculated by the following equation:

$$\% \text{ U removal} = ((C_o - C_e) / C_o) \times 100 \quad (1)$$

Where:  $C_o$  was the initial concentration of uranium and  $C_e$  was the concentration of uranium at equilibrium.

The adsorption capacity  $q_e$  ( $\text{mg g}^{-1}$ ) after equilibrium was calculated by mass balance relationship equation as follows:

$$Q_e = ((C_o - C_e) / W) \times V \quad (2)$$

Where: V was the volume of the solution and W was the mass of adsorbate.

All data are presented as mean  $\pm$  standard deviation (SD) unless otherwise stated. Error bars in the figures represent the SD of at least three independent experiments.

### III. RESULTS AND DISCUSSION

#### Characterization of potato peels (PP)

##### Infrared spectroscopy analysis (FTIR)

FTIR is a widely utilized method for identifying the chemical functional groups present in a compound. As shown in Figure (2a), Strong peaks were found at  $3450\text{ cm}^{-1}$  attributed to presence of  $-\text{OH}$  stretch of the phenol group in cellulose and lignin. Also, peak at  $2930\text{--}2854\text{ cm}^{-1}$ , respectively corresponding to the  $-\text{CH}$  and  $-\text{CH}_2$  stretch of the aliphatic molecule. Furthermore, the peaks at  $1735$  and  $1636\text{ cm}^{-1}$  corresponding to  $\text{C}=\text{O}$  stretch of the aldehyde group and the  $\text{C}=\text{C}$  stretch of the phenol group, respectively. Popuri et al. [17, 18]. Moreover,  $1507$ ,  $1370$ ,  $892$ , and  $660\text{ cm}^{-1}$  attributed to  $\text{N-H}$  deformation,  $\text{C-O-H}$  bend,  $\text{C-N}$  stretch, and  $\text{C-O-H}$  twists, respectively. Ghodbane et al. [19].

##### X-ray diffraction

Figure (2b), illustrates the X-ray diffraction pattern of the potato peel as received. From the XRD founded that PP represent amorphous structure with  $2\theta \approx 20$  with high intensity.

##### EDX and SEM Analysis

EDX analysis of Potato peel represent in Figure (2c) and SEM micrographs of Potato peel represent in Figure (2d). Images magnification of  $500\times$  was carried out. The preparation process of the potato peel resulted in a rough and porous surface indicated that improved adsorption on its surface.

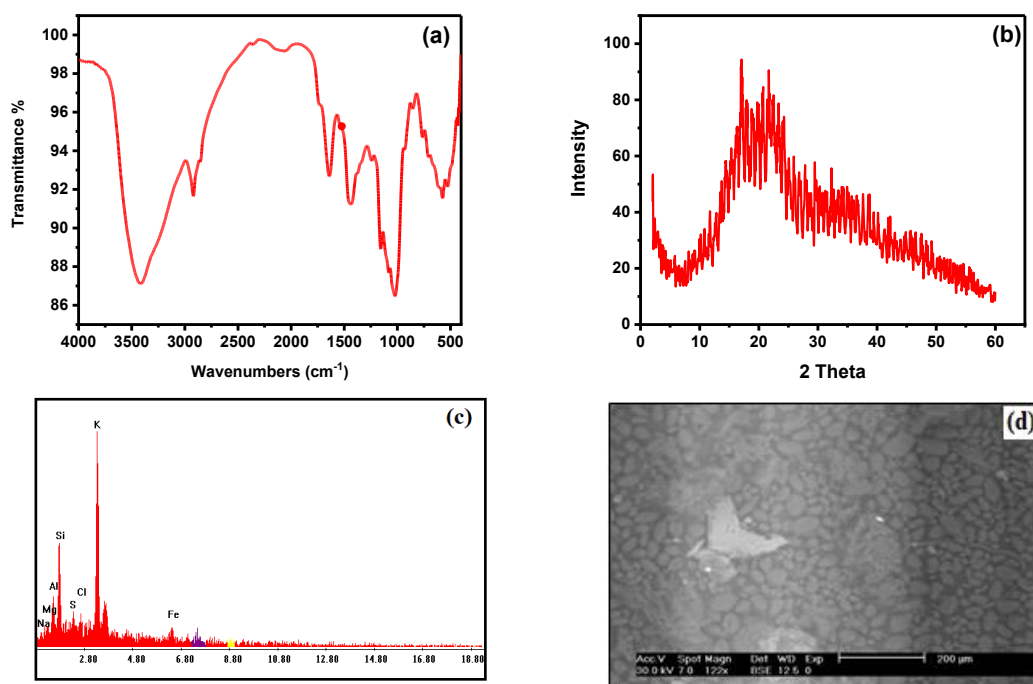


Figure 2: (a) FTIR, (b) XRD, (c) EDX and (d) SEM spectra micrographs of PP

##### Determination of point of zero charge ( $\text{pH}_{\text{PZC}}$ )

The  $\text{pH}_{\text{PZC}}$  of the pp was determined by using  $0.01\text{ M NaCl}$  solution, at  $298\text{ K}$ . In different 100 conical flask,  $50\text{ ml}$  of the  $0.01\text{ M NaCl}$  solution was added and the  $\text{pH}$  was adjusted at 2, 3, 4, 5, 6, 8 and 10 using  $0.5\text{ M HCl}$  or  $0.5\text{ M NaOH}$ . Then  $0.05\text{ gm}$  of pp was added to each of the above  $\text{pH}$  adjusted solutions and equilibrated for 24 h. the final  $\text{pH}$  values of the solution were recorded and the difference between the initial and final  $\text{pH}$  ( $\Delta\text{pH}$ ) was plotted against the initial  $\text{pH}$  values. The PZC values were calculated from  $\Delta\text{pH}$  plot, at the  $\text{pH}$  where  $\Delta\text{pH}=0$ . In the current study, the  $\text{pH}_{\text{PZC}}$  of pp was calculated using the  $\text{pH}$  drift method Figure 3 represents a graph of  $\Delta\text{pH}$  vs initial  $\text{pH}$ , and the  $\text{pH}_{\text{PZC}}$  of pp was determined to be  $5.01\pm 0.2$ .

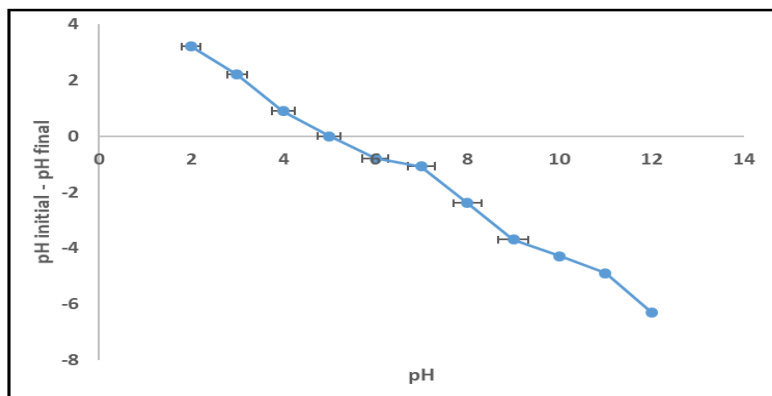


Figure 3: Point of zero charge ( $pH_{PZC}$ ) for Potato peel.

### Characterization of mixture

#### Infrared spectroscopy analysis (FTIR)

Figure 4 show the FTIR (4 a) for the adsorption effects represent in, the peak represented at 2376, 1890, 1242, 1110, 1076, and 957  $cm^{-1}$  after U(VI) adsorption assigned to N–H stretch, C=O Stretch of ketone group, Si–C stretch, C–O–C asymmetric stretch, P–H deformation or C–O stretch, and Si–OH asymmetric stretch. Furthermore, the intensity of the peak shifted to lower values after U(VI) adsorption indicated that the adsorbent changes the peaks, which reflects the PP's complex composition. K. M.et al. [20].

#### X-ray diffraction

Figure (4b) represented that shifting  $2\theta$  to lower values  $\approx 18$ , with lower in its intensity after sorption. This data proves that adsorption occurs at the surface affected by the chemical and physical properties of the adsorbate and adsorbent. Moreover, Potato peels (PP) were subjected to adsorption studies with a number of factors, including temperature, pH, adsorbent quantity, and time effects, were optimized.

#### SEM micrographs

Figure (4 c) shows that the presence of uranium in the composite led to change its surface with increase in uranium concentration which present in EDX (4c) spectra proves that adsorption occurred very well in the presence of potato peel.

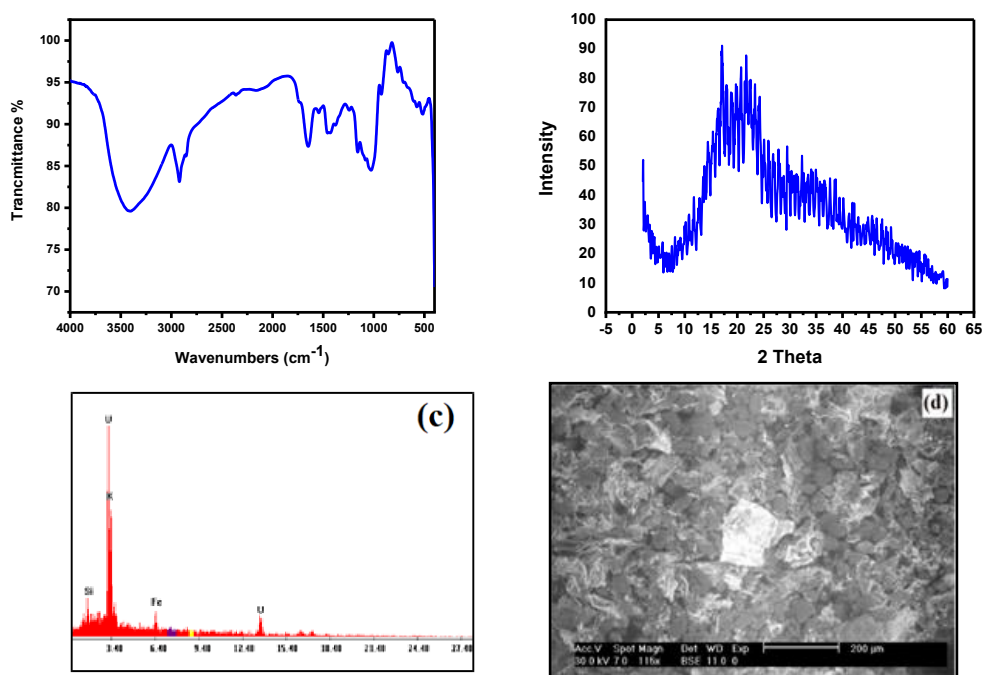


Figure 4: (a) FTIR, (b) XRD, (c) EDX and SEM spectra micrographs of PP+U

### Surface area analysis

The surface characteristics of pp were determined using the BET method as displayed in Table (1). Specific surface area values of 8.2591 m<sup>2</sup> /g were detected for the presented adsorbent. After adsorption, the detected BET-specific surface area of the spent adsorbent was found to be 17.0254 m<sup>2</sup> /g, confirming the efficient uptake of uranium ions by the introduced adsorbent in current research work. Marwa et al. [21].

**Table 1:** Surface area analysis of PP sorbent before and after U(VI) sorption process.

Sample	Specific surface area, m <sup>2</sup> /g	Total pore volume, cc/g	Average pore radius, nm
PP	8.2591	0.0142999	1.92029
PP+ U	17.0254	0.0305011	1.92681

### Zeta potential

The average zeta potential measurement of pp before and after U(VI) sorption process are collected in Table (2). The zeta potential analysis reveals significant changes in surface charge characteristics of the PP biosorbent following U(VI) adsorption. The untreated PP exhibited a strongly negative zeta potential of -45.31 mV, reflecting the abundance of anionic functional groups (e.g., carboxylate, phenolate) on its surface. This negative charge facilitates initial U(VI) in UO<sub>2</sub><sup>2+</sup> cation attraction through electrostatic interactions. After U(VI) sorption, the zeta potential shifted dramatically to +13.31 mV, indicating successful UO<sub>2</sub><sup>2+</sup> binding and surface charge reversal, Al-Ghamdi et al., [22, 23]. The positive shift suggests: (1) coordination of positively charged uranyl ions (UO<sub>2</sub><sup>2+</sup>) with oxygen-containing groups, (2) potential formation of uranium hydroxo complexes at the surface, and (3) possible precipitation of uranium species that alter the interfacial charge distribution, Al-Ghamdi et al., [22]. Moreover, the observed shifts in cell current (from 0.98 to 0.92 mA) and frequency (from -3.69 to +1.36 Hz) confirm significant surface modification during adsorption. The charge reversal suggests a dual adsorption mechanism: initial electrostatic attraction followed by stronger coordination complexes or surface precipitation Al-Ghamdi et al., [22].

**Table 2:** Average zeta potential and relative indices of PP sorbent before and after U(VI) sorption process.

Sample	Cell current, mA	Frequency Shift, Hz	Avg. Mobility, M. U.	Avg. Zeta Potential, mV
PP	0.98	-3.69	-3.17	-45.31
PP+U	0.92	1.36	0.93	13.31

### Effect of uranium solution media:

The performance of the adsorption procedure was significantly impacted by the study solution medium. It is beneficial to find the appropriate adsorption media with a high rate of adsorption. An examination of this parameter in the context of an industrial adsorption process may lead to energy and financial savings. To evaluate the media on the adsorption of U (VI) ions on PP, H<sub>2</sub>SO<sub>4</sub> and HCl have been used. From the obtained results founded that elimination of U (VI) was higher in HCl media than H<sub>2</sub>SO<sub>4</sub>, it reached 61.5±1.9% in HCl versus 10±.43% in H<sub>2</sub>SO<sub>4</sub>. Although the additional adsorbent medium increased the available surface area and the active sites increased, we used HCl media in all of our investigations from an economic perspective, which led to a high percentage of metal removal.

### Effect of pH

The initial pH of solutions containing metal ions is one of the primary parameters determining metal adsorption processes. This is because hydrogen ions have a strong affinity for a large number of ion exchange and complexing sites. Sole' et al. [24]. However, the hydrogen ion may compete with the positively charged metal ions on the adsorbent's active sites. El-Khamssa et al. [25].

The effect of pH on the adsorption of U(VI) ions on PP has been examined by varying pH between 1 and 5, as shown in Figure 5 (a). This pH range (pH <5) was chosen to avoid metal precipitation Parida et al. [26, 27]. Figure 5 (a), shows that adsorption of U(VI) ion increased and achieves its maximum adsorption effectiveness of (70.8±3.54)% at pH 4.0 ± 0.11 attributed to ion exchange and hydrogen bonding occurs due to presence of a number of elements present in PP composition and complexing properties, with increase in pH values (4-5), adsorption gradually shifted to lower values due to more negative charges and fewer protons.

It is believed that the pH affects the adsorption kinetics due to the electrostatic interaction between the adsorbent surface and the U(VI) ions in solution, as shown in Figure 5 (a) It arises from differences in the surface charges of adsorbents at different pH values and variations in uranium speciation. From literature review founded that at pH values higher than 5, U(VI) Hydrolyzed and precipitated. Furthermore, at pH values between (4 – 5), yield and uranium adsorption efficiency gradually decreased attributed to presence of anionic uranium species (UO<sub>2</sub>Cl<sup>-</sup>) which are prevalent in this region within precipitate and hydrolyze at pH values higher than 5.

### Effect of adsorbent dose

Optimizing adsorption efficiency is essential because it is influenced by both sorbent mass and sample volume. Figure 5 (b) represent effect of bio-sorbent dosage at different masses in 10 mL with an initial uranium (VI) concentration of  $100 \text{ mg L}^{-1}$  to identify the ideal solid-liquid phase most efficiently. It showed that adsorption reach it is maximum values up to  $\approx 0.05$  from PP dosage then start to decrease gradually and level off this attributed to agglomeration and/or aggregation may occur at higher concentration of PP which would decrease the effective surface area and availability of active bio-sorbent centers for uranium bio-sorption Ghodbane et al. [28, 29]. This method is both economically and environmentally justified because the adsorption efficiency values did not change considerably at different solid-liquid phase ratios. The results showed that the highest uranium adsorption capability, up to  $80 \pm 2.93\%$ , was found in  $0.05 \pm 0.004 \text{ g}$  of potato peel.

### Effect of initial concentration

Using the best experimental settings previously evaluated and a range of U (VI) concentrations ( $25\text{--}400 \pm 5.3 \text{ mg L}^{-1}$ ), a series of batch experiments were conducted to investigate the effect of the initial concentration factor. Figure 5(c) represent the relationships between the initial uranium content and the adsorption effectiveness of the (PP) bio-sorbent using chloride media. It is obvious from the data that adsorption increase and ability of PP to adsorb up to  $95.75 \pm 4.79\%$  of U (VI) on chloride media.

This is due to the enhanced powerful strength of the concentration gradient and can be explained as follows: At low adsorbent ratios, the PP structure has several adsorption sites, with an increase in adsorbent ratios cause adsorption sites to become saturated, which reduces adsorption effectiveness Ghodbane et al. [28, 29].

### Effect of Contact Time

Figure 5 (d), represent the effect of contact time on U(VI) adsorption, the pH was raised to 4 with an initial concentration  $C_0$  of  $100 \pm 3 \text{ mg L}^{-1}$  and  $0.05 \pm 0.004 \text{ g}$  of PP at  $25^\circ\text{C}$ . At the first five minutes were spent reaching adsorption equilibrium, after which it increase for the next fifty to sixty minutes reaches its equilibrium around 60 minutes, as well as, almost all of the U(VI) ions were adsorbed after 60 minutes for the majority of the adsorption to be completed.

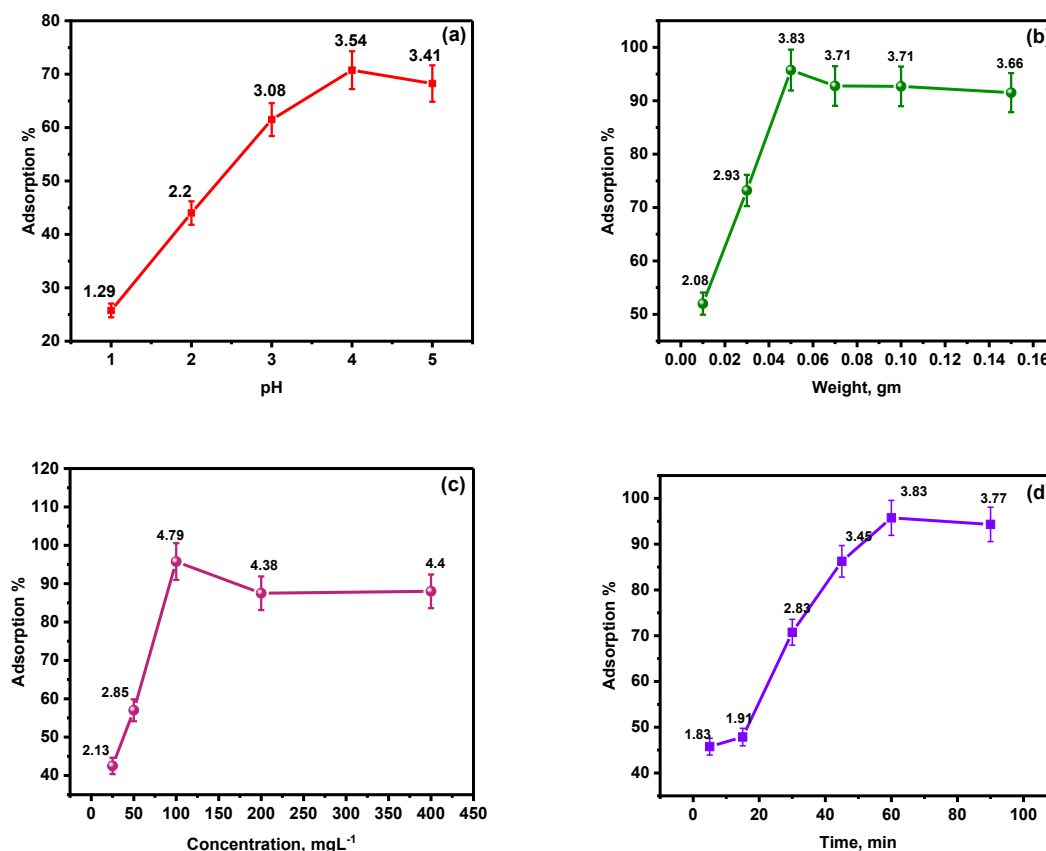


Figure 5: (a) Effect of pH on the uranium (VI) ions uptake by PP at initial concentration of  $100 \text{ mgL}^{-1}$  at time 60 minutes at temperature  $25^\circ\text{C}$ , (b) Effect of potato peel dose on adsorption of U (VI) ions at initial concentration of  $0.1 \text{ gL}^{-1}$  at time 60 minutes at temperature  $25^\circ\text{C}$ , (c) Effect at initial concentration of U(VI) ions at time 60

minutes at temperature 25°C and (d) Effect of contact time of U(VI) adsorption, at pH 4±0.11 with an initial concentration 100±3 mg L<sup>-1</sup> and 0.05±0.004 g of PP at 25°C.

The interaction mechanism between hydroxyl active sites and uranium (VI) positive charge species may include their coordination modes. Nonetheless, the coordination of the UO<sub>2</sub><sup>2+</sup> ions is dominated by the donor atoms (four, five, or six). Therefore, the anticipated mechanism of the reaction between (PP) and the uranium ions represented in Figure 6, which shows that the quantities of [Cl]<sup>-1</sup> required to achieve chemical equilibrium at a concentration of 1 ml of [UO<sub>2</sub>]<sup>+2</sup>. It was discovered that the optimal pH for the interaction of uranium ions with PP at 25°C was 4±0.11.

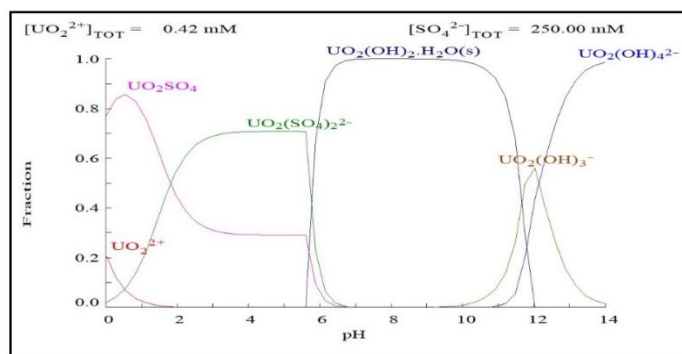


Figure 6: The concentrations of [Cl]<sup>-1</sup> required for chemical equilibrium to occur when concentration of 1 mM of [UO<sub>2</sub>]<sup>+2</sup>

All experiments were repeated and analyzed three time, we used average in the figures.

### Kinetic Studies

To learn more about the mechanism of adsorption through kinetic studies, the experimental data of uranium ion adsorption by PP were evaluated using a pseudo-first order and a pseudo-second order kinetic model of Equations 1 and 2.

Pseudo-first-order Damiyine et al. [30]:  $\text{Log}(q_e - q_t) = \text{Log}q_e - t(K_1/2.303)$  (1)

Pseudo-second-order Fayoud et al. [31]:  $t/q_t = 1/K_2q_e^2 + (1/q_e)t$  (2)

Where:  $q_t$  (mg. g<sup>-1</sup>) and  $q_e$  (mg.g<sup>-1</sup>) the adsorption capacity of uranium ions at time  $t$  and at equilibrium,  $k_1$  (min<sup>-1</sup>) and  $k_2$  (g.mg<sup>-1</sup>.min) the rate constants of pseudo-first order and pseudo-second order models respectively. Based on the regression coefficient ( $R^2$ ) values of the pseudo-first order and pseudo-second order kinetic model equations' linear plots, as displayed in Figure 7, the best-fit model was selected.

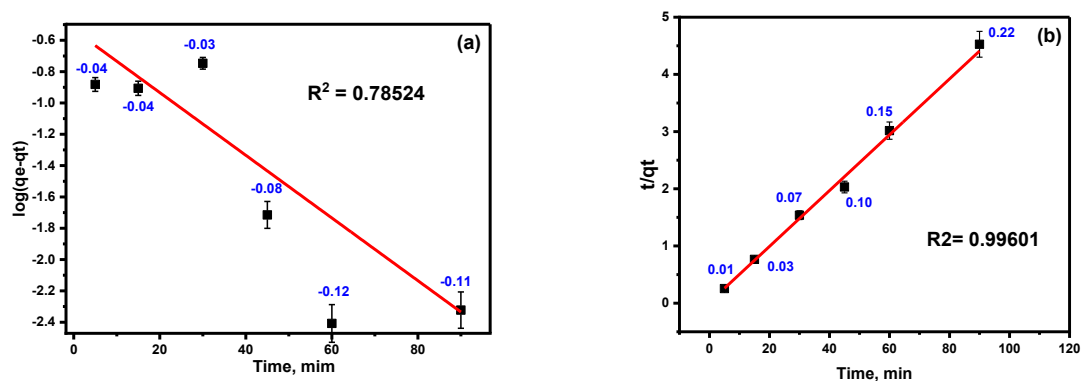


Figure 7: (a) Pseudo-first-order and (b) Pseudo-second kinetics of U(VI) adsorption by potato peels from the synthetic hydrochloric acid [100±3 mg L<sup>-1</sup> of U(VI)] at 25°C

### Isotherm Studies

To gain a better understanding of the adsorption capacity, the PP adsorption capacity was assessed using various isotherm models, including the Freundlich and Langmuir models. The Langmuir isotherm indicates that adsorption takes place at homogenous adsorption sites on the sorbent and that intermolecular interactions quickly decrease as one moves away from the adsorption surface. Equation 3 is the expression for the Langmuir model and the data presented in Figure 8 (a) Abd El Fatah et al. [32].

$$\frac{C_e}{q_e} = \frac{C_e}{q_{max}} + \frac{1}{K_L q_{max}} \quad (3)$$

Where:  $C_e$  was the equilibrium concentration of uranium ions in solutions ( $\text{mg L}^{-1}$ ),  $q_e$  was the amount adsorbed on PP at  $C_e$  ( $\text{mg g}^{-1}$ ),  $Q_{\text{max}}$  was the maximum adsorption capacity ( $\text{mg g}^{-1}$ ), and  $K_L$  was the Langmuir binding constant related to adsorption energy ( $\text{L mg}^{-1}$ ).

The earliest known relationship characterizing non-ideal and reversible adsorption is the Freundlich isotherm model, which may be extended to multilayer adsorption under the assumption of energy surface heterogeneity. The Freundlich isotherm model shown in Figure 8 (b) and represented by equation (4) which are nonlinear and linear, respectively.

$$\log q_e = \log K_f + \frac{\log C_e}{n} \quad (4)$$

Where:  $K_f$  and  $n$  were the Freundlich constants for adsorption capacity and intensity, respectively,  $K_L$ ,  $Q_{\text{max}}$ ,  $K_f$ , and  $n$  were the values were obtained.

The maximal Langmuir adsorption capabilities ( $Q_{\text{max}}$ ) generated were in good agreement with the experimental ones, and the values of  $R^2$ , a measure of goodness of fit, support the idea that the Langmuir model better fits the experimental data than the Freundlich model. The linear method yielded higher  $R^2$  values for the Freundlich isotherm parameters than the non-linear least squares method. Furthermore, Figure 8 represented that Langmuir isotherm models is higher than that of Freundlich models when these models are compared, proves that the homogeneity of the active sites on the PP surface.

The Temkin model states that the adsorption heat decreases linearly with surface coverage due to the interaction between the adsorbent and the adsorbate and can be expressed as follows Temkin et al. [33]:

$$q_e = a \ln K_T + a \ln C_e \quad (5)$$

Where:  $K_T$  was the equilibrium parameter with regard to the maximum binding energy ( $\text{L/g}$ ), and  $A$  was the dimensionless constant related to temperature and adsorption system.

The Temkin isotherm constants,  $a$  and  $K_T$ , can be found using the slope and intercept of the plot of  $q_e$  vs.  $\ln C_e$ , as shown in Figure 8 (c). The D-R isotherm suggests that the adsorbent's porosity dictates the characteristics of the adsorption curves, and the equation can be expressed as follows:

$$\ln q_e = \ln q_{\text{DR}} - \beta \varepsilon^2 \quad (6)$$

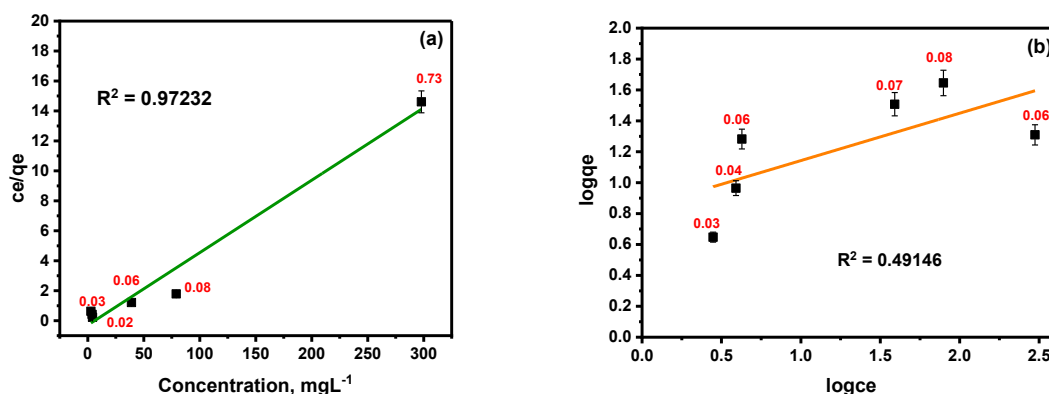
$$\varepsilon = RT \ln (1 + 1/ C_e) \quad (7)$$

$$E = 1/ \sqrt{2\beta} \quad (8)$$

Where:  $q_{\text{DR}}$  was the theoretical monolayer adsorption capacity ( $\text{mol/g}$ ),  $\beta$  ( $\text{mol}^2/\text{J}^2$ ) was the D-R constant related to adsorption energy,  $\varepsilon$  ( $\text{J}^2/\text{mol}^2$ ) was the Polanyi potential, and  $E$  was the mean adsorption energy that gives useful information about chemical and physical adsorption ( $\text{kJ/mol}$ ).

The type of adsorption is estimated by the free energy ( $E$ ) in the D-R isotherm; however, physical adsorption is taken into consideration when the  $E$  value is less than  $8 \text{ kJ/mol}$ . The  $E$  value between  $8$  and  $16 \text{ kJ/mol}$  shows the chemical ion exchange mechanism of adsorption Esra et al. [34]. The  $E$  value for the selected study is  $0.387667 \text{ kJ/mol}$ . These findings showed that the adsorption of  $\text{U(VI)}$  onto the prepared sample is a physical process, as shown in Figure 8 (d).

The characteristics of the Freundlich, Temkin, Langmuir, and D-R isotherms are displayed in Table 3, which demonstrates that the correlation coefficient  $R^2$  values are poorly fitted when compared to the Langmuir. The expected amount of uranium as a function of the weight of PP was calculated given the actual uranium ion concentrations in solution. This implies that it is theoretically possible to determine the necessary PP weight before the adsorption procedure for any concentration range. The Langmuir model's applicability explains how uranium adsorbs in a monolayer on the uniform surface of PP



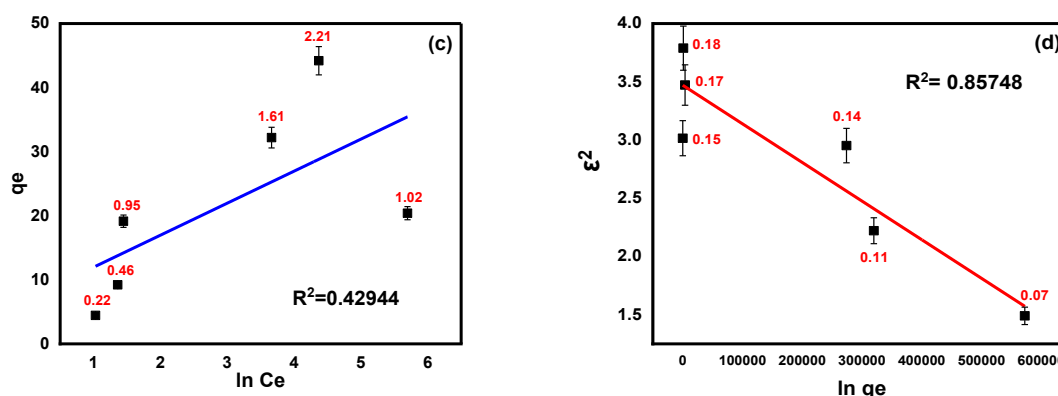


Figure 8: (a) Langmuir plot, (b) linear Freundlich plot, (c) Temkin and (d) D–R isotherm of the adsorption of uranium ions on Potato Peels

**Table 3:** Estimated isotherm parameters for the U(VI) adsorption on PP

Model	Parameter	Value ( $\pm 0.01:2.2$ SD)
Langmuir	$q_{max}$ (mg/g)	20.66
	$K_L$ (Lmg <sup>-1</sup> )	0.16
	$R^2$	0.97
Freundlich	$N$	3.30
	$K_f$	2.29
	$R^2$	0.49
Temkin	$KT$	4.06
	$A$	4.84
	$R^2$	0.43
D–R	$q_{DR}$ (mg/g)	11.49
	$\beta$ (mol <sup>2</sup> /J <sup>2</sup> )	3.33
	$R^2$	0.86
	$EDR$ (kJ/mol)	0.39

In recent years, potato peel wastes have been employed for the production of bio-sorbents which are used for the treatment of effluents and various other contaminated sources i.e. pigments, dyes, metals. Although, an updated list concerning specifically Potato peel waste is here presented. With almost no cost what-so-ever, potato peel can undergo several treatments leading to materials with specific properties for a precise adsorbate. Numerous studies have been published which prove the efficiency as well as the efficacy of potato peels for this perspective. However, the most recent achievements in this subject are illustrated in Table (4).

**Table 4:** List of adsorbents and respective potato peel waste treatment Ali et al. [35].

Adsorbate	Potato peel waste treatment	Maximum adsorbent capacity	References
Cr (VI) ions	Untreated	1.97 mg/g	Mohammed et al.[36]
As & F	Untreated	2.17 $\mu$ g/g & 2.91 mg/g	Bibi et al.[37]
Cu (II)	Untreated	84.74 mg/g	Kyzas et al.[38]
Ni (II)	Untreated	2.702 mg/g	Mahale et al.[39]
Cr (IV)	Hydrochloric acid Untreated	3.28 mg/g	Mutongo et al.[40]

U(IV)	19.15±0.74 mg/L	This study
-------	-----------------	------------

### Thermodynamics Studies

Conducting adsorption experiments at four different temperatures enables us to determine the set of thermodynamic parameters of the adsorption procedure, such as enthalpy ( $\Delta H^\circ$ ), Gibbs free energy ( $\Delta G^\circ$ ) and entropy ( $\Delta S^\circ$ ) for adsorption using the following equations (10, 11) Liang et al. [41, 42].

$$\log K_e = \frac{\Delta S^\circ}{2.303R} - \frac{\Delta H^\circ}{2.303RT} \quad (10)$$

$$\Delta G^\circ = \Delta H^\circ - T\Delta S^\circ \quad (11)$$

Here the adsorption affinity constant,  $K_e = (Q/C_e)$ , and  $C_e$  is the concentration (mg/L) of the U(VI) at equilibrium. The enthalpy and entropy can be calculated from the slope and intercept of the straight line resulting from plotting  $\log K_e$  vs  $1/T$  Figure 9. Substituting these values into equation (11) Mona et al. [43]. From Table 5, which represented various thermodynamic parameters at different temperature showed that the enthalpy of adsorption ( $\Delta H^\circ$ ) that physisorption also takes part in adsorption process in which the adsorbate adheres to the surface only through weak intermolecular interactions. The negative value of free energy change ( $\Delta G^\circ$ ) is an indication of a spontaneous process whereby no energy input from outside of the system is required. However, the values of ( $\Delta G^\circ$ ) decreased with increasing temperature, indicating that adsorption of U (VI) ions on PP became less favorable at higher temperature. The negative value of entropy change ( $\Delta S^\circ$ ) shows a decreased disorder at the solid/liquid interface during U(VI) adsorption. As the temperature increases, the mobility of U(VI) ions increases causing the ions to escape from the solid phase to the liquid phase. Therefore, the amount of U(VI) that can be adsorbed will decrease Ngah et al. [44].

**Table 5:** shows the Values of thermodynamic parameters:

T (K)	$\Delta G^\circ$ (kJ mol <sup>-1</sup> )	$\Delta H^\circ$ (kJ mol <sup>-1</sup> )	$\Delta S^\circ$ (J.mol <sup>-1</sup> .K <sup>-1</sup> )
298	-4399.73	-164360	-536.781
313	968.0731	-164360	-536.781
313	6335.88	-164360	-536.781
323	11703.69	-164360	-536.781

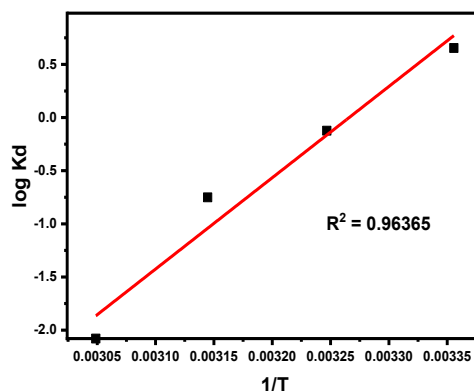


Figure 9: Effect of temperature on the adsorption efficiency of uranium ions on potato peel

### Adsorbent Regeneration

Desorption studies are critical for evaluating adsorbent performance, particularly regarding elution efficiency, regeneration capability, and reuse potential Hyun Park et al. [45]. The desorption mechanism often mirrors adsorption processes, potentially involving ion exchange or complexation reactions when treating metal-loaded adsorbents with deionized water Eloh et al. [46]. In this study, U(VI) desorption was achieved through 60-minute equilibrium treatment using 0.1N HCl at a fixed adsorbent concentration (1 g L<sup>-1</sup>), with desorption efficiency monitored at 10-minute intervals. The material demonstrated exceptional recyclability, maintaining over 93±3.2% adsorption efficiency through five consecutive adsorption-desorption cycles with only ~6.9% capacity loss. Remarkably, the adsorbent showed stable performance beyond the fifth cycle with no significant degradation, indicating excellent chemical stability for repeated applications.

### Real application- Monazite leachate liquor

Adsorption studies were conducted using acidic leachates derived from monazite ore specimens collected from the Abou-Kashaba coastal region (black sand deposits) near Rosetta, Egypt (Rashid City, Beheira Governorate). Monazite, an orthophosphate mineral bearing rare earth elements (REEs) and thorium, was characterized for its composition and physical properties. Quantitative analysis revealed the Egyptian monazite sample (97% purity) contained  $\text{ThO}_2$  (5.9%),  $\text{U}_3\text{O}_8$  (0.44%),  $\text{Ce}_2\text{O}_3$  (26.55%), with remaining REE oxides ( $\text{RE}_2\text{O}_3$ ) constituting 34.35% of the total composition. The monazite dissolution was performed using the conventional industrial hydrothermal autoclave method with concentrated sulfuric acid (98%  $\text{H}_2\text{SO}_4$ ). In a typical procedure, 100 g of monazite ore was digested with 90 mL of concentrated  $\text{H}_2\text{SO}_4$ . Subsequent dilution with distilled water yielded 1 L of leachate solution, achieving approximately 85% dissolution efficiency, while the remaining 15% constituted insoluble residue after filtration Abd El Fatah, A.I. L. [47]. The resulting sulfate leach liquor, representing the most economical approach for monazite decomposition, was then used for uranium adsorption studies. Prior to adsorption experiments, the leachate was treated with NaOH to precipitate dissolved species at pH 9, followed by filtration to obtain a clear solution for subsequent resin testing. Following dissolution of the precipitate with HCl, the solution was diluted with 500 mL of deionized water.

The resulting hydrous cake contained multiple metal ions with the following composition:  $\text{UO}_2^{2+}$  (0.491%),  $\text{La}^{3+}$  (18%),  $\text{Ce}^{3+}$  (31.79%),  $\text{Pr}^{3+}$  (7.43%),  $\text{Nd}^{3+}$  (15.41%),  $\text{Sm}^{3+}$  (5.06%),  $\text{Gd}^{3+}$  (4.67%), and  $\text{Th}^{4+}$  (1.273%). For uranium sorption studies, 500 mL of the acidic monazite leachate (pH 4.0, room temperature) was contacted with 1.0 g of PP adsorbent for 60 minutes. After reaching equilibrium, the mixture was filtered and the residual uranium concentration was analyzed. Comprehensive characterization using FTIR, SEM, and EDX confirmed the uranium adsorption capacity and mechanism. As demonstrated in Figures 10 (a-c), the adsorption studies in chloride media revealed a uranium uptake efficiency of  $51.13 \pm 1.8\%$  by PP. Notably, the presence of  $\text{Th}^{4+}$  in the system was found to influence the adsorption behavior.

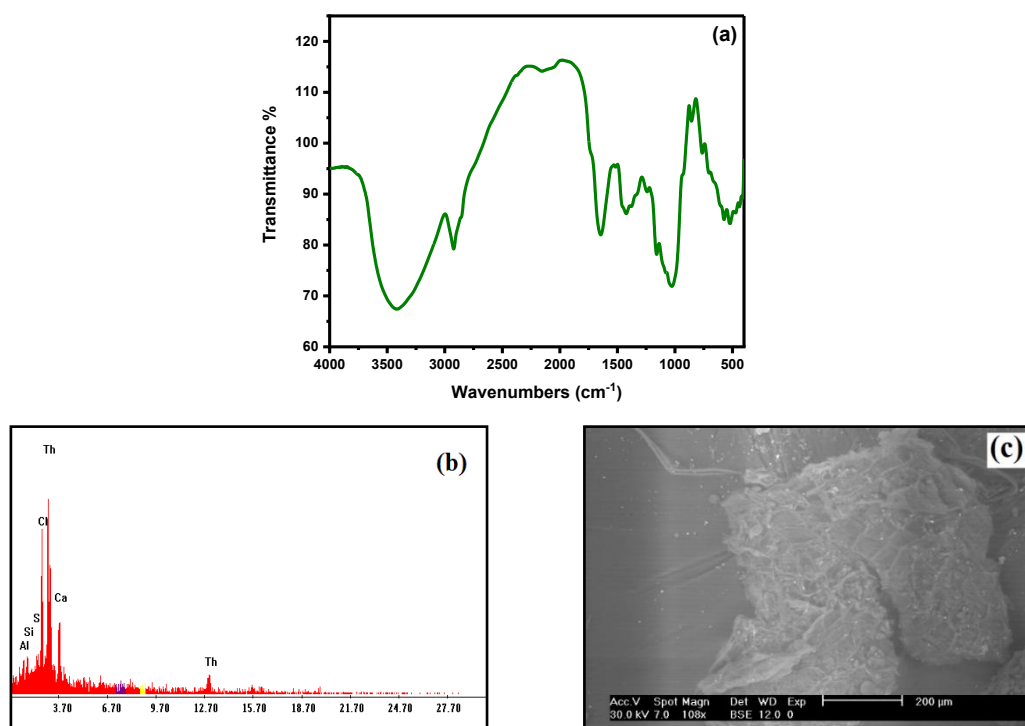


Figure 10: (a) FTIR, (b) EDX and (c) SEM spectra micrographs of PP+U from Leach liquor

### CONCLUSIONS

This study demonstrates the effective utilization of potato peel (PP) as a sustainable biosorbent for U(VI) removal from aqueous solutions. FTIR analysis confirmed the presence of hydroxyl ( $-\text{OH}$ ), carboxyl ( $-\text{COOH}$ ), and amine ( $-\text{NH}_2$ ) functional groups on PP, which facilitate U(VI) binding via complexation and ion-exchange Silva, et al., [48,49]. Adsorption efficiency increased with higher initial U(VI) concentration ( $25\text{--}400 \pm 5.3$  mg/L), optimal pH ( $4.0 \pm 0.11$ ), and adsorbent dosage ( $0.05 \pm 0.004$  g), following pseudo-second-order kinetics ( $R^2 > 0.99$ ), indicative of chemisorption-dominated mechanisms. While intraparticle diffusion contributed to the adsorption process, external mass transfer and surface interactions also governed the rate-limiting steps. Equilibrium data aligned with the Langmuir isotherm, revealing homogeneous monolayer adsorption with a maximum capacity

of  $19.25 \pm 0.74$  mg/g at  $25^\circ\text{C}$ . These findings position PP as a low-cost, renewable adsorbent for uranium remediation, with potential for scalability in wastewater treatment systems. Furthermore, the thermodynamic analysis confirms the exothermic nature of U(VI) adsorption onto potato peel ( $\Delta H^\circ = -164.36$  kJ/mol), with positive entropy change ( $\Delta S^\circ = -536.78$  J/mol·K) indicating increased disorder at the solid-liquid interface during adsorption Smith, et al. (50). The negative Gibbs free energy values ( $\Delta G^\circ = -4399.73$  kJ/mol) demonstrate spontaneous adsorption. These findings, coupled with the demonstrated adsorption capacity ( $19.25 \pm 0.74$  mg/g) and selectivity in acidic conditions, position potato peel as a viable, low-cost biosorbent for uranium recovery from acidic monazite leachates. In the current work, we employed PP byproduct, which contains a high concentration of organic compounds without any modifications, as an adsorption system to investigate its impact on the adsorption process for the batch technique of uranium removal from aqueous solutions. Additionally, forecast the ideal conditions for various pH, time, temperature, and uranium concentrations.

## REFERENCES

- [1]. Alqadami, AA, Naushad, M, Alothman, ZA, Ghfar, AA, ACS Appl Mater Interfaces, 2017. 9:36026–36037. <https://doi.org/10.1021/acsami.7b10768>.
- [2]. Abdi, S, Nasiri, M, Mesbahi, A, Khani, MH. J. Hazard Mater, 2017. 332:132–139. <https://doi.org/10.1016/j.jhazmat.2017.01.013>
- [3]. Ding, S, Yang, Y, Li C, Huang, H, Hou, L. Water Res, 2016. 95:174–184. <https://doi.org/10.1016/j.watres.2016.03.028>
- [4]. Chen, QY., Yao, Y., Li, XY., Lu, J., Zhou, J., Huang, ZL. J Water Process Eng, 2018. 26:289–300
- [5]. Onorato, C, Banasiak, LJ, Schafer, AI. Sep Purif Technol, 2017. 187:426–435. <https://doi.org/10.1016/j.seppur.2017.06.016>
- [6]. Shasha, Y., Yiwei, H., Guolin, H., Wei, P., Chenglun, G., Jeffery, S., Received: 30 December 2019 / Published online: 17 March 2020 © Akadémiai Kiadó, Budapest, Hungary 2020.
- [7]. Ecaterina, M., Maria, R., Andra Mihaela P., Anca Andreea T., Ruxandra V., Cristian P., Constantin B., Liliana B., and Cristina O., Materials. 2021, 14, 4581. <https://doi.org/10.3390/ma14164581>
- [8]. Yusuf, M. Handb. Ecomater. 2017, 1–11. Doi: 10.1007/978-3-319-48281-1\_48-1
- [9]. Jagtap, S., Bhatt C., Thik, J., Rahimifard, S. Sustainability. 2019, 11, 3173. Doi:10.3390/su11113173
- [10]. Selvendran et al., Alka Gupta and Tripti Verma ISSN: 1994, 2319-7706 Volume 9 Number 10. 2020, Int.J.Curr.Microbiol.App.Sci. 2020, 9(10): 546-553.
- [11]. Kyzas, G.Z., Bomis, G., Kosheleva, R.I., Efthimiadou, E.K., Favvas, E.P., Kostoglou, M., Mitropoulos, A.C. Chem. Eng. J. 2019, 356, 91–97. Doi:10.1016/j.cej.2018.09.019.
- [12]. Gutha, Y., Munagapati, V.S., Naushad, M., Abburi, K. Desalination Water Treat. 2015, 54, 200–208, Doi:10.1080/19443994.2014.880160
- [13]. El-Azazy, M., El-Shafie, A.S., Issa, A.A., Al-Sulaiti, M., Al-Yafie, J., Shomar, B., Al-Saad, K. J. Chem. 2019. Doi:10.1155/2019/4926240. 2019
- [14]. Kyzas, G.Z., Deliyanni, E.A., Matis, K.A. Colloids Surf. A Physicochem. Eng. Asp. 2016, 490, 74–83. Doi:10.1016/j.colsurfa.2015.11.038.
- [15]. Guechi, E.-K., Hamdaoui, O. Desalination Water Treat. 2016, 57, 10677–10688, Doi:10.1080/19443994.2015.1038739.
- [16]. Ahsan, J., Awais, A., Ali, T., Umair, S., Muhammad, N., Adeela, H. AIMS Agriculture and Food. 2019. Volume 4, Issue 3: 807-823. Doi: 10.3934/agrfood.2019.3.807.
- [17]. Popuri, Srinivasa Reddy, Kvn, Kalyani, s., Abburi & Krishnaiah. Wood Science and Technology. 2007, Volume 41(5):427-442. Doi:10.1007/s00226-006-0115-4.
- [18]. Hameed, B.H., Mahmoud, D.K., Ahmad, A.L. J. Hazard. Mater. 2008. 158, 65–72.
- [19]. Ghodbane, I., Nouri, L., Hamdaoui, O., Chiha, M. J. Hazard. Mater. 2008, 152, 148–158.
- [20]. Parida, K.M., Amaresh, C.P. Journal of hazardous materials. 2010. 173, 758. Doi: 10.1016/j.jhazmat.2009.09.003. Epub 2009 Sep 4.
- [21]. Marwa, El A., Ahmed, S El-S., Ahmed, A I., Maetha Al-S., Jawaher, Al-Y., Basem, S., and Khalid, Al-S. Journal of Chemistry Volume, 2019, Article ID 4926240, 14pages. <https://doi.org/10.1155/2019/4926240>.
- [22]. Al-Ghamdi, A.A., Galhoum, A.A., Alshahrie, A., Al-Turki, Y.A., Al-Amri, A.M., Wageh, S. Polymers.2022, 14: 2568.
- [23]. Imam, E.A., Hashem, A.I., Tolba, A.A., Mahfouz, M.G., El-Sayed, I.E.-T., Hawash, H.B., Neiber, R.R., Mira, H.I., Galhoum, A.A., Guibal, E. Sep. Purif. Technol. 2023, 323: 124466.
- [24]. Sole, M., Casas, J.M., Lao, C. Air Soil Pollut. 2003, 144, 57–65.
- [25]. El-Khamssa, G., Oualid, H. Badji Mokhtar-Annaba University, 21 Apr. 2015. P.O. Box 12, 23000 Annaba, Algeria, Tel./ Fax: +213 38876560 Published online:
- [26]. Parida, K. M., Pradhan, A. C. Journal of hazardous materials. 2010, 173, 758.
- [27]. Damiyine, B., Guenbour, A., Boussen, R. Journal of Materials and Environmental Science. 2017, 8 (1), 345.
- [28]. Ghodbane, I., Hamdaoui, O. J. Hazard. Mater. 2008, 160, 301–309.
- [29]. Hameed, B.H., El-Khaiary, M.I. J. Hazard. Mater. 2008, 157, 344–351.
- [30]. Damiyine, B., Guenbour, A., Boussen, R. Journal of Materials and Environmental Science. 2017, 8 (1),345.
- [31]. Fayoud, N., Alami, Y. S., Tahiri, S., Albizane, A. J. Mater. Environ. Sci. 2015, 6 (11), 3295.
- [32]. Abd El Fatah, A. I. L., Soaad, M., Elashry. Journal of Inorganic and Organometallic Polymers and Materials.2022. <https://doi.org/10.1007/s10904-022-02344-7>
- [33]. Temkin, M.J. Pyzhev, V. Acta physicochim. 1940, USRR121, 217-222.
- [34]. Esra, B., Mustafa, T., Ahmet, S. Journal of Environmental Radioactivity. 2017, 175-176, 7-14.
- [35]. Ali, T., Umair, S., Muhammad, N., and Adeela, H. AIMS Agriculture and Food. 2019, Volume 4, Issue 3: 807-823. Doi: 10.3934/agrfood.2019.3.807
- [36]. Mohammed, NMS., Salim, HAM., Sci J Uni Zakho. 2017, 5: 254-258. Doi: 10.25271/2017.5.3.392
- [37]. Bibi, S., Farooqi, A., Yasmin, A., et al. Int J Phytoremediat, 2017, 19: 1029-1036. Doi: 10.1080/15226514.2017.1319329.
- [38]. Guechi, EK., Hamdaoui, O. Desalin Water Treat. 2016, 57: 10677-10688.
- [39]. Mahale, KK, Mokhasi, HR., Ashoka, H., et al. Res J Chem Environ Sci. 2016, 4: 96-101.
- [40]. Mutongo, F., Kuipa, O., Kuipa, PK., et al. Bioinorg Chem Appl, 2014, 2014: 1-7.
- [41]. Liang, S., Guo, X., Feng, N., Tian, Q. J. Hazard. Mater. 2010, 174, 756–762.
- [42]. Mata Y.N., Blázquez M.L., Ballester A., Gonzez F., Munoz J.A. J. Chem. Eng. 2009, 150 289–301.

- [43]. Mona, T., Al-Shemy, A., Al-Sayed, A., Sawsan, D. Separation and Purification Technology, 2022, 290, 120825
- [44]. Ngah, W., Megat H. & Megat Ahmad K. Biochemical Engineering Journal. 2008, 39. 521–530. Doi:10.1016/j.bej.2007.11.006
- [45]. Hyun Park, Ju., Sholom, W., Mitchell, H G., Ulrike, P., Kevin, B J., , Nilanjan, C. Nature Genetics. July 2010, 42(7):570-5. Doi:10.1038/ng.610
- [46]. Elo, N., Silke, S. J. of Hazardous Materials. 2012. Doi: **10.1016/j.jhazmat.2012.01.084**
- [47]. Abd El Fatah, A.I. L. International Journal of Science and Research (IJSR) ISSN. 2019. 1989.2319-7064 SJIF: 7.583-Volume 10 Issue 3, March. 2021. Doi: 10.21275/SR21316221646.
- [48]. Silva, M. , Oliveira, P., Santos, A. Food Chemistry. 2023, 415(Part 2), 135890. <https://doi.org/10.1016/j.foodchem.2023.135890>
- [49]. Kumar, V., Kumar, A., Singh, J. International Journal of Biological Macromolecules, 2022, 218, 1081-1090. <https://doi.org/10.1016/j.ijbiomac.2022.08.064>
- [50]. Smith, J., Jones, L. *Journal of Chemical Thermodynamics*, 2021, 158, 106452. <https://doi.org/10.1016/j.jct.2021.106452>.